



*Conference Proceedings of the 5th Asia Pacific Luminescence and Electron Spin Resonance Dating Conference
October 15th-17th, 2018, Beijing, China*

Guest Editor: Grzegorz Adamiec

ESR CHRONOLOGY OF BEDROCK FAULT ACTIVITY IN CARBONATE AREA: PRELIMINARY RESULTS FROM THE STUDY OF THE LIJIANG-XIAOJINHE FAULT, SOUTHEASTERN TIBET, CHINA

GONGMING YIN¹, CHUNRU LIU¹, RENMAO YUAN¹, FEI HAN¹,
RUI DING^{1,2} and JEAN-JACQUES BAHAIN³

¹State Key Laboratory of Earthquake Dynamics, Institute of Geology, China Earthquake Administration, Beijing 100029, China

²Key Laboratory of Crustal Dynamics, Institute of Crustal Dynamics, China Earthquake Administration, Beijing 100085, China

³UMR 7194 HNHP, Département Homme et Environnement du Muséum National d'Histoire Naturelle,
1 rue René Panhard, 75013 Paris, France

Received 4 February 2019

Accepted 3 March 2020

Abstract: Carbonated rocks constitute one of the main lithologies of the southeastern Tibet area, China, a tectonically very active zone. However, due to the lack of suitable dating materials, it is difficult to carry out chronological studies of the local tectonic evolution in such carbonate areas. In the present study, electron spin resonance (ESR) method had been applied on the dating of carbonates heated during fault activity of the Lijiang-Xiaojinhe (LX) Fault, an important active fault located in the northwest of Yunnan Province. Clear displaced landforms show that the fault has undergone strong late-Quaternary activity. During the fault activity, the heat produced by friction lead to the melting of the frictional surface of the rocks, and the melting can attenuate or zero the ESR dating signal of carbonate. The aim of the present paper was to check the ability of carbonate use to chronologically identify fault activity using electron spin resonance (ESR) method. The results showed the last fault activity of the LX fault was dated by ESR about 2.0 ± 0.2 ka ago, in agreement with historical and radiocarbon data. Hence ESR can be if necessary a practicable dating alternative method for the study of fault activity chronology in carbonate rock area.

Keywords: ESR, carbonate, Lijiang-xiaojinhe fault, resetting by heating/melting.

1. INTRODUCTION

The southeastern margin of the Tibet Plateau, which is one of the important areas for the study of active tectonics, is marked by the presence of numerous faults

having played in relation with the regional tectonic activity. Carbonated rocks constitute one of the main lithologies of this area, and it is difficult to carry out chronological surveys of the local tectonic evolution in such carbonated areas due to the lack of suitable dating materials. In the present paper, we have checked the ability of recrystallized carbonate use to chronologically identify fault activity using electron spin resonance (ESR) method.

Corresponding author: GM Yin
e-mail: yingongming@ies.ac.cn

As early as the 1970s, Ikeya (1975) made the first ESR dating study of carbonates using stalactite calcite. The results being encouraging, the ESR dating method was subsequently developed and applied rapidly on different Quaternary materials, including carbonates from marine or continental origin (e.g., Smith *et al.*, 1985; Chen *et al.*, 1987; Molodkov, 1988; Yin *et al.*, 2001; Li *et al.*, 2015).

Thermal annealing experiments show that heating (over 200°C) can attenuate or zero the ESR dating signal of carbonate (e.g. Yokoyama *et al.*, 1983; Bahain *et al.*, 1994; Pirouelle *et al.*, 2007; Diao *et al.*, 2018). As a great deal of heat is produced during the fault activity process, the ESR dating signal in carbonate rocks could decay or clear up in relation with this heating. Therefore, it seems theoretically possible to study fault activity in carbonate rock area by ESR method.

Here the preliminary results of the ESR study of fault activity in carbonated area are displayed for the Lijiang-Xiaojinhe fault, China.

2. GEOLOGICAL SETTING AND SAMPLING

The Lijiang-Xiaojinhe (LX) Fault is an important active fault located in the northwest of Yunnan Province, and its length is about 400 km (Xiang *et al.*, 2002). LX fault locates along the boundary of the northwest Sichuan and central Yunnan sub-blocks in the Sichuan-Yunnan block in eastern Tibet. LX fault is not only the main boundary fault controlling the steep deformation zone of the southeastern margin of the Qinghai-Tibet Plateau but also the main transverse fault in the Sichuan-Yunnan rhombic block. Clear displaced landforms show that the fault has undergone strong late Quaternary activity (Cheng *et al.*, 2012). There have been many earthquakes in this area. However, fewer materials can be used to measure the age of fault activity in such carbonate rock area.

During the fault activity, the heat produced by friction leads to the melting of the frictional surface of the rocks. The thickness of the molten layer, often about a few millimetres, is then related to the intensity of the tectonic movement and associated temperature increase. As LX fault is developed in carboniferous limestone with a fracture bandwidth of about 20 meters, the main slip surface is a smooth fault triangle on the surface of which a thin layer of carbonate newly formed by friction and scratches can be observed. In this study, we have picked the carbonate material on the frictional surface of the LX fault, in order to try to date its last tectonic activity and associated intensity, see Fig. 1 and Fig. 2.

The carbonate sample has been divided into three parts following their external aspects: fully melted (A), partially modified (B), and slightly or not modified (C), see Fig. 2(3). The observed modifications of the carbonate rock structure were interpreted as the results of the heating of the carbonate rock during the fault movement.

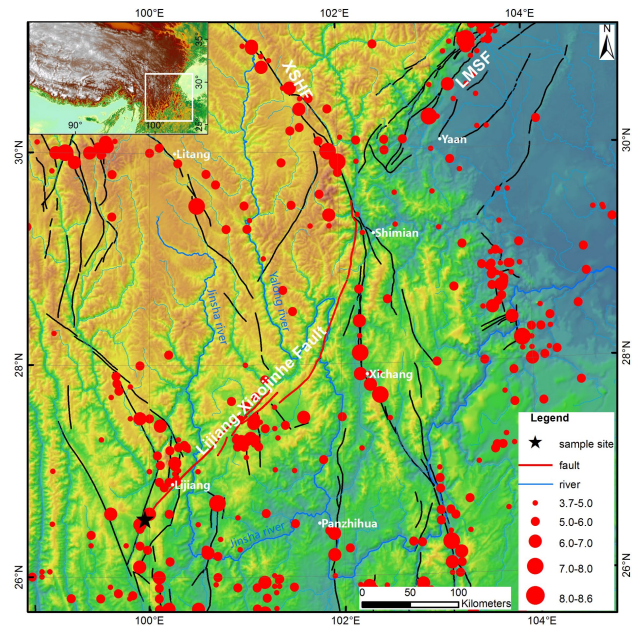


Fig. 1. Location of the Lijiang-Xiaojinhe fault, southeastern Tibet. The red dots denote earthquakes, and the size of red dots denotes magnitude. The sample site is indicated by a black star.

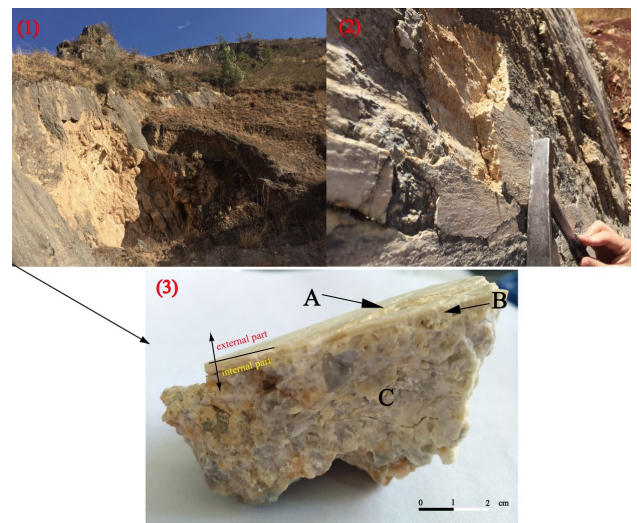


Fig. 2. Global (1) and detailed (2) views of the sampling area. Picture (3) is the photo of carbonates sample with indication of the sampling point (red square) on picture (1). Area A: milky white and be melted again thoroughly; area B: yellow-white and be partially melted; area C: grey-green and has not the characteristic of being melted.

When the fault is active, the limestone on the fault plane receives high-speed friction producing an increase of the temperature, which leads to the carbonate melting again thoroughly and forming a new milky white layer (part A of our sample), which is smooth and a thin plate shape with a thickness of about 1–2 mm. Yellow-white part B, rough and globular, belongs to the material of fault fracture zone adjacent to part A. Part B seems have been

partially melted and re-cemented under the action of the fault activity in relation with a thermal effect. In opposition, grey-green Part C looks similar with original carboniferous limestone and seems unmodified, without any characteristic of melted rocks.

3. EXPERIMENTAL METHODS

Sample preparation and irradiation

The three aforementioned parts of the sample (A, B, C) were separated and similarly crushed, the 100–200 μm grain size fraction of each part was then selected, dried after cleaning with distilled water and divided into several 200 mg aliquots. These aliquots have received additional gamma doses ranging from 0 to 400 Gy using the ^{60}Co gamma source of Peking University.

Measurement of the dose rate

The dose rate was calculated using the dose conversion factors of Guerin *et al.* (2011) from the concentrations of uranium, thorium and potassium of each sample determined by ICP-MS analyses. The cosmic dose rate was calculated on the burial depth of the sample from the Prescott and Hutton (1994).

ESR measurement

ESR signal intensities were measured by a BRUKER ER041XG X-band spectrometer at room temperature, using microwave power of 0.01 mW, the centre field of 351.4 mT, sweep width 15 mT, modulation frequency 100 kHz, and modulation amplitude 0.1 mT, in the ESR laboratory of the Institute of Geology, China Earthquake Administration, Beijing, China. All of the samples were measured three times with different directions to obtain the average intensity. Fig. 3 showed ESR spectra of the

LX fault nature sample (part C). A prominent feature is the presence of the hyperfine sextet associated with Mn^{2+} nuclear spin ($I=5/2$) and associated forbidden transition lines ($\Delta m=\pm 1$). The intensity of Mn^{2+} signals is strong in calcite because of the repulsion of Mn^{2+} in the recrystallization of CaCO_3 during stalactite growth (Ikeya, 1993).

In our samples, the ESR intensity of additional radiation-induced signals (located in the spectrum area between Mn^{2+} peaks 3 and 4) in the natural sample was relatively weak although it should have been exposed to natural radiations for several million years. However, it is difficult to create defects in the carbonate with a high impurity content as the inactive volume around Mn^{2+} , Fe^{2+} , and Al^{3+} in the calcite lattice absorbs radiation energy (*i.e.*, creates electrons and holes) without forming stable defects (Ikeya, 1993).

It is better to select a stable radio-sensitive signal increasing in intensity with artificial irradiation for ESR dating (Henning and Grün, 1983). In our samples, we observed three ESR peaks at $g=2.0006$, $g=2.0039$, and $g=2.0057$ respectively, which have practically been used as a dating signal (signal A, B and C of Ikeya and Ohmura (1981), linked to freely rotating SO_2^- , axial SO_3^- and freely rotating CO_2^- respectively) (Barabas, 1992; Debuyst *et al.*, 1990), see Fig. 4. The thermal stabilities of these three signals can be classified as following: $g=2.0057 > g=2.0039 > g=2.0006$, characteristics observed in carbonates samples from different origins (Bahain *et al.*, 1994). According with its relatively low thermal stability, ESR intensity of the $g=2.0006$ line can be bleached to zero over 200°C according to the isochronal annealing curve (Ikeya, 1993). Parallel, the signal intensity increases obviously with added artificial irradiation doses. Therefore, we selected the $g=2.0006$ ESR signal as the dating signal in this study.

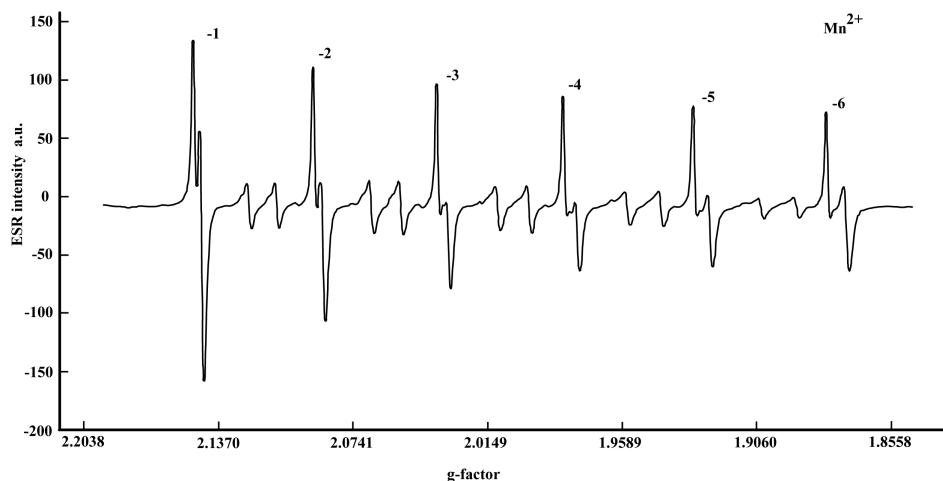


Fig. 3. ESR spectra of the LX fault nature sample (part C).

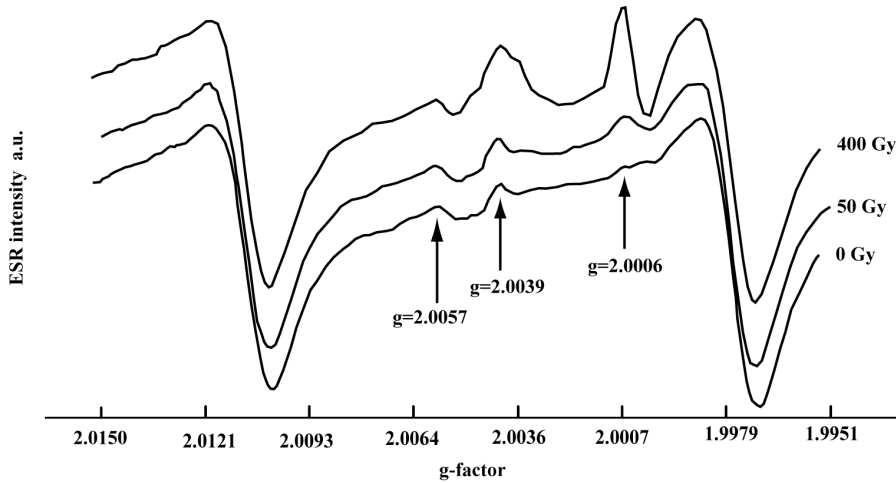


Fig. 4. ESR spectra of the LX fault sample (part C) for different artificial irradiation doses.

4. RESULTS AND DISCUSSION

Thermal effect on ESR signal

The apparent characteristics of the samples seem to show different degrees of thermal effect, so will their ESR signals show the same characteristics? Fig. 5 compare the natural ESR spectra of parts A, B and C. It shows clearly the same ESR characteristic Mn^{2+} -3 and Mn^{2+} -4 peaks, and the three dating signals (at $g=2.0057$, $g=2.0039$, $g=2.0006$) whose intensities decrease gradually from part C to B to A. These intensity changes of the three sample parts are consistent with their supposed heating: higher the heating temperature, greater the attenuation of ESR signal. The friction surface (part A) has received the biggest thermal effect because the temperature of the frictional surface is the highest when the fault is active, then part of the thermal effect is received by part B, which was close to part A. On the other hand, the influence of fault activity on part C is weak.

As Mn^{2+} is not radio-sensitive, the signal decrease observed from part C to A could be related to different Mn

contents of the three parts and not to a thermo-sensitivity. Therefore, we had quantified the Mn contents of the different parts of the LX fault sample by LA-ICP-MS at the State Key Laboratory of Earthquake Dynamics, Institute of Geology, China Earthquake Administration. Sample ablations were performed using a Resolution M50 ArF excimer laser at a wavelength of 193 nm. An Agilent 7900 quadrupole ICP-MS was used to determine the ion signal intensities under argon gas. Helium gas and aerosolized samples were mixed with Ar/N₂ gas via a T-connector before entering the ICP-MS. Nitrogen was added to enhance the sensitivity of the ICP-MS, reduce the background and lower the polyatomic ion interference (Pang *et al.*, 2017). The results show that if Mn content decreases gradually from part C to B to A, the measured content changes are quite restricted (about 7.6 and 2.4 ppm respectively for part B and A against 9.5 ppm in Part C). Comparing with part C, the ESR signal intensities of Mn^{2+} -3 and Mn^{2+} -4 in part B attenuate to 24% and in part A attenuate to 6%. As Part A and B show melting characteristics and usually the melting also affects the

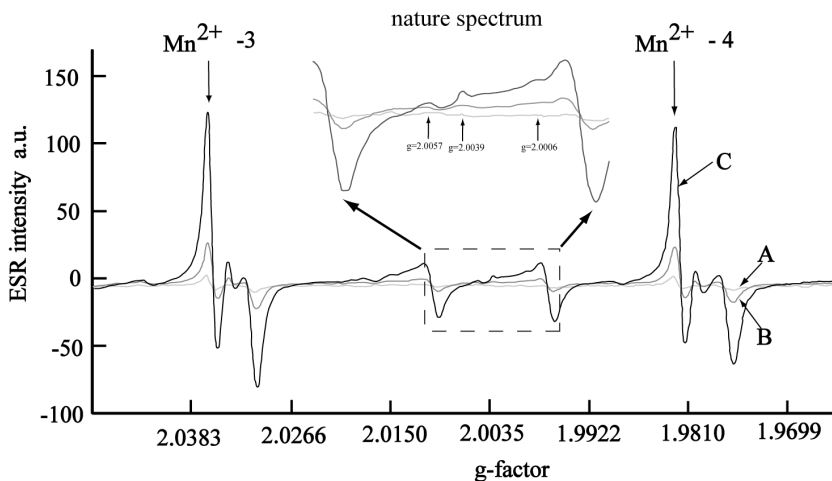


Fig. 5. Natural ESR spectra of LX samples (part A, B and C). Mn^{2+} -3 at $g=2.0345$ and Mn^{2+} -4 at $g=1.9804$ are two of the six main peaks of the Mn^{2+} ESR spectrum in calcite.

number of available traps in manganese lattices, it seems that both content change and melting attenuate the ESR intensity of Mn^{2+} in LX samples from part C to A.

Equivalent dose

The dose response curves of $g=2.0006$ peak were established for Parts A, B and C, and the equivalent doses (De) were obtained from the ESR intensities-doses data set by extrapolation. For all subsamples, the equivalent doses values and their individual errors were determined from the dose response data fitted with a linear function. The obtained dose response curves are displayed in Fig. 6.

The obtained equivalent doses for parts A, B and C are 1.9 ± 0.2 , 2.1 ± 0.2 and 4.6 ± 0.4 Gy, respectively. We can notice that the equivalent doses are consistent for parts A and B within the error, while the equivalent dose determined for part C is much bigger.

Dose-rate and age calculation

In order to obtain the age, the dose rate has been calculated. Because the composition of carbonate rock is homogeneous and part A and B are thinner (about a few millimetres), we have considered that the three part (A, B and C) have been submitted to the same dose rate. The content of uranium, thorium and potassium of the LX sample were determined by chemical method (ICP-MS) as 0.099 ± 0.005 ppm, 0.192 ± 0.010 ppm and $0.045\pm 0.002\%$ respectively. The cosmic dose rate was estimated at 0.287 ± 0.011 Gy/ka (the burial depth set to 35–40 cm). From these data, the dose rate of carbonate rock was estimated at 1.074 ± 0.050 Gy/ka, see Table 1. The ages of the last tectonic activity recorded into parts A and B are 1.77 ± 0.2 ka and 1.96 ± 0.2 ka respectively. An average age of 1.87 ± 0.2 ka can be calculated. The detail information see Table 1.

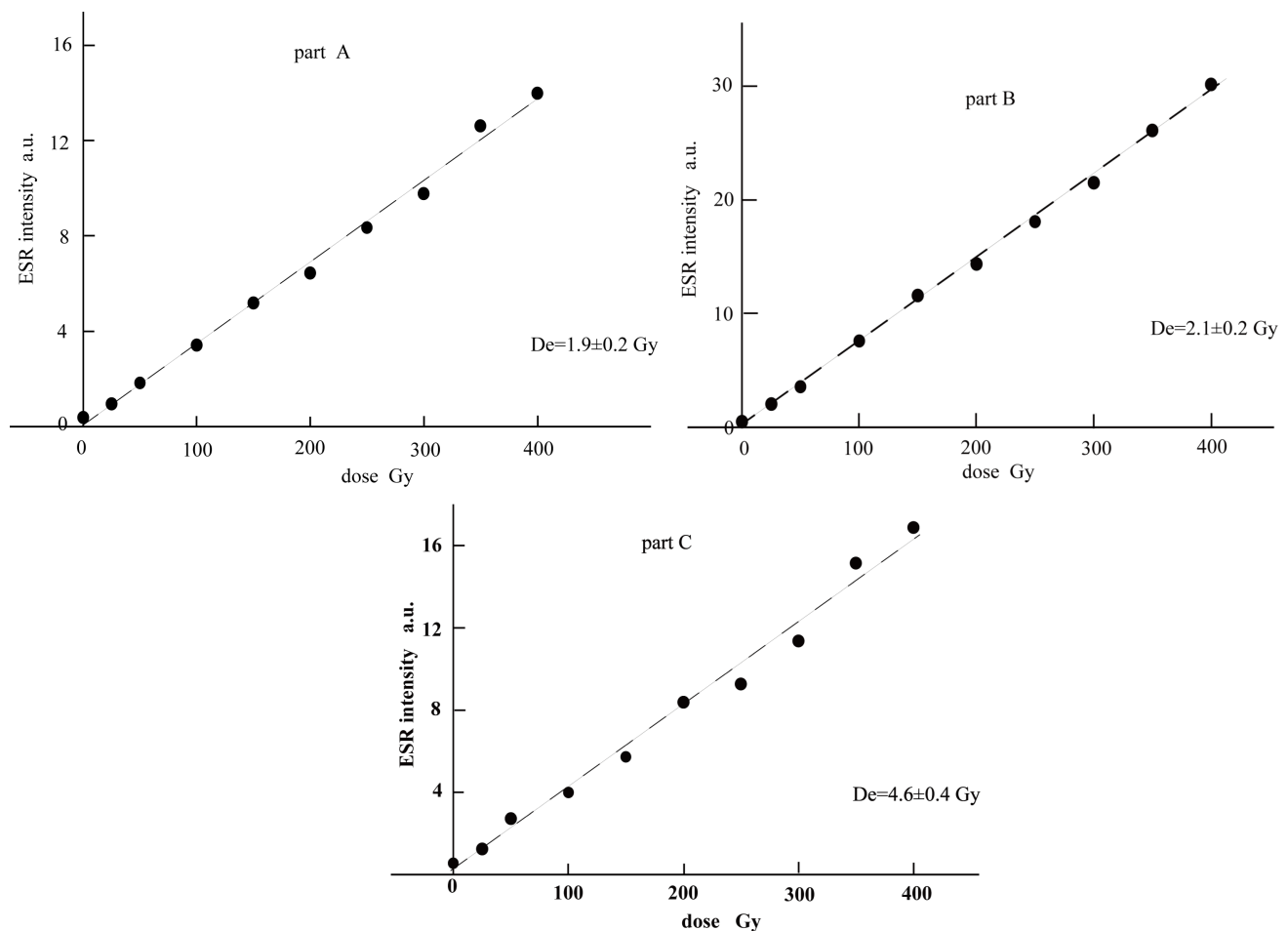


Fig. 6. Dose response curves of the $g=2.0006$ line for LX samples.

Table 1. ESR dating results of the LX fault.

Sample	Depth (m)	U ($\mu\text{g/g}$)	Th ($\mu\text{g/g}$)	K (%)	cosmic dose rate (Gy/ka)	D (Gy/ka)	De (Gy)	Age (ka)
part A							1.90 \pm 0.20	1.77 \pm 0.20
part B	0.30	0.099 \pm 0.005	0.192 \pm 0.010	0.045 \pm 0.002	0.287 \pm 0.011	1.074 \pm 0.050	2.10 \pm 0.20	1.96 \pm 0.20
Part C							4.60 \pm 0.40	4.28 \pm 0.40

5. DISCUSSION

Practical ESR dating on carbonates started in the 1970–1980s on stalactites and stalagmites in caves. Radiation-induced defects in carbonates have been well identified by more recent investigations in the 1990s using synthetic carbonates doped with impurities and ^{13}C -isotope. Although there are some problems and limitations, ESR has given overall reliable ages of crystallization of calcite using signals due to CO_2^- and SO_3^- . The ESR age is then deduced from equivalent dose extrapolated from the dose-response curve and from dose rate deduced from the contents of ^{238}U , ^{232}Th and ^{40}K using the method of radiation assessment.

In the middle segment of the Lijiang-Xiaojinhe fault area, three trenches were excavated on the basis of high resolution satellite image interpretation, and the age of the last paleoearthquakes was constrained by radiocarbon dating and OxCal 4.3 modelling (more details see https://c14.arch.ox.ac.uk/oxcalhelp/hlp_contents.html). It indicated that three tectonic events occurred on the middle segment of the LX Fault during the Holocene at 7940~7210a Cal BP, 4740~4050a Cal BP and 1830~1540a Cal BP, respectively. Large earthquakes on the middle segment of the LX fault appear to fit the quasi-periodic model with a mean recurrence interval of ~3000a and an estimated 7.5 magnitude (Ding *et al.*, 2018).

In the present study, the ESR dating results of carbonate samples collected from fault slip surface (1.77 to 1.96 ka) could correspond to the impact of the latest paleoearthquake event (1830~1540 a Cal BP), which shows that the dating signal seems have been reset by the heating related to the fault friction and ESR could be systematically used to estimate the age of the last tectonic event recorded in the carbonated area. In fact, as landslides often occur in the limestone area, and as molten carbonate layer can be formed on the slip surface of the landslide that is similar to fault slip surface. It also seems possible to determine the occurrence time of landslide events.

6. CONCLUSION

In this study, several carbonate samples related to the tectonic movements of the Lijiang-Xiaojinhe fault were studied by ESR in order to estimate the quality of the thermal resetting of the carbonates due to the tectonic

activity as well as the age of the last recorded tectonic event.

- 1) The friction surface melts and recrystallizes when the fault is active, which can reset the ESR dating $g=2.0006$ signal of calcite to zero.
- 2) The last fault activity of the LX fault is dated by ESR about 1.85 \pm 0.2 ka ago, so in relatively good agreement with the last historical recorded Earthquake (dated by radiocarbon between 1830 and 1540a Cal BP). ESR can therefore provide a practicable dating method for the study of fault activity in carbonate rock area. Of course, on the reliability and accuracy of the ESR dating results, further research is needed.

ACKNOWLEDGEMENTS

This research was supported by the State Key Laboratory of Earthquake Dynamics, Institute of Geology, China Earthquake Administration (Grant No.LED2016A01) and National Nonprofit Fundamental Research Grant of China, Institute of Geology, China, Earthquake Administration (Grant No. IGCEA1908). We are grateful to senior engineer Haijun Yang, Analysis Center, Department of Chemistry, Tsinghua University, for discussion. We thank Dr. Jianzhang Pang for the elemental analysis of LA-ICP-MS at Institute of Geology, China Earthquake Administration. We would also like to thank Prof. Jiu-Qiang Li for his support with the ^{60}Co irradiation at Peking University.

REFERENCES

- Bahain JJ, Yokoyama Y, Masaoudi H, Falguères C and Laurent M, 1994. Thermal behaviour of ESR signal observed in various natural carbonates. *Quaternary Science Reviews* 13: 671–674, DOI 10.1016/0277-3791(94)90096-5.
- Barabas M, 1992. The nature of the paramagnetic centres at 2.0057 and 2.0031 in marine carbonates. *Nuclear Tracks and Radiation Measurements* 20: 453–464.
- Chen YJ, Lu JF, Cai TM, He RG and Zhang RL, 1987. ESR dating of cave secondary carbonates *Georeview* 33(4): 339–345.
- Cheng J, Xu XW, Gan WJ, Ma WT, Chen WT and Zhang Y, 2012. Block model and dynamic implication from the earthquake activities and crustal motion in the southeastern margin of Tibetan plateau. *Chinese Journal of Geophysics* 55(4): 1198–1212, DOI 10.6038/j.issn.0001-5733.2012.04.016 (in Chinese).
- Debuyst R, DeCanniere P and Dejehet F, 1990. Axial CO_2^- in α -particle irradiated calcite: potential use in ESR dating. *Nuclear Tracks And Radiation Measurements* 17: 525–530.
- Diao SB, He XL, He LL, Zhang DL, Zhang J and Li JP, 2018. Thermodynamic properties of ESR signals of deep-sea carbonate. *Marine Geology Frontiers* 38(8): 1–6.

- Ding R, Ren JJ, Zhang SM, Lv YW and Liu HY, 2018. Late quaternary paleoearthquake on the middle segment of the Lijiang-Xiaojinhe fault, southeastern Tibet. *Seismology and Geology* 40(3): 622–640.
- Guérin G, Mercier N and Adamiec G, 2011. Dose-rate conversion factors: update. *Ancient TL* 29(1): 5–8.
- Henning GJ and Grün R, 1983. ESR Dating in Quaternary Geology. *Quaternary Science Reviews* 2: 157–238.
- Ikeya M, 1975. Dating a stalactite by electron paramagnetic resonance. *Nature* 255: 48–50, DOI 10.1038/255048a0.
- Ikeya M and Ohmura K, 1981. Dating of fossil shells with electron spin resonance. *Journal of Geology* 89: 247–250, DOI 10.1086/628583.
- Ikeya M, 1993. *New application of electron spin resonance dating, dosimetry and microscopy*. World Science Publishing Co. Pte. Ltd., 1–500.
- Li JP, Diao SB, Liu CR, He XL and Zhang DL, 2015. The application of ESR dating to marine carbonate. *Marine Geology Frontiers* 31(10): 65–70.
- Molodkov A, 1988. ESR dating of quaternary shells: recent advances. *Quaternary Science Reviews* 7: 477–484, DOI 10.1016/0277-3791(88)90049-2.
- Pang JZ, Zheng DW, Ma Y, Wang Y, Wu Y, Wan JL, Yu JX, Li YJ and Wang YZ, 2017. Combined apatite fission-track dating, chlorine and REE content analysis by LA-ICPMS. *Science Bulletin* 62: 1497–1500, DOI 10.1016/j.scib.2017.10.009.
- Pirouelle F, Bahain JJ, Falguères C and Dolo JM, 2007. Study of the effect of a thermal treatment on the D_E determination in ESR dating of speleothems. *Quaternary Geochronology* 2: 386–391, DOI 10.1016/j.quageo.2006.05.030.
- Prescott JR and Hutton JT, 1994. Cosmic ray contributions to dose rates for luminescence and ESR dating: Large depths and long-term time variations. *Radiation Measurements* 23(2–3): 497–500, DOI 10.1016/1350-4487(94)90086-8.
- Smith BW, Smart PL and Symons CR, 1985. ESR signals in a variety of speleothem calcites and their suitability for dating. *Nuclear Tracks and Radiation Measurements* 10: 837–844, DOI 10.1016/0735-245X(85)90098-5.
- Xiang HF, Xu XW, Guo SM, Zhang WX, Li HW and Yu GH, 2002. Sinistral thrusting along the Lijiang-Xiaojinhe Fault since Quaternary and its geologic-tectonic significance: Shielding effect of transverse structure of intracontinental active block. *Seismology and Geology* 24(2): 188–198 (in Chinese).
- Yin GM, Sun YJ, Ye YG and Liu W, 2001. The ESR age of shells from the bed of Dali with human fossil. *Acta Anthropologica Sinica* 20(1): 34–38.
- Yokoyama Y, Quaegebeur JP, Bibron R and Léger C, 1983. ESR dating of Paleolithic calcite: Thermal annealing experiment and trapped electron life time. *PACT* 9: 371–379.